Pergamon

Cement and Concrete Research 32 (2002) 615–621

CEMENT AND CONCRETE RESEARCH

Effect of superfine slag powder on cement properties

Quanlin Niu[a,*], Naiqian Feng[a], Jing Yang[a], Xiaoyan Zheng[b]

[a]*School of Civil Engineering, Tsinghua University, Room 239, Building 1, Beijing 100084, China*
[b]*China Building Material Academy, Beijing 100024, China*

Received 6 November 2000; accepted 5 November 2001

Abstract

The particle size distribution (PSD) of the dense packing powder and that of actual cement powder was analyzed to explain the packing effect of superfine powder. The degrees of hydration of slag powders with specific surface area ranging from 300 to 800m^2/kg were calculated to illustrate the enhancement of pozzolanic effect. As an examination of the analysis, blended cement mortars and pastes incorporating superfine slag powder were tested for strength and mercury intrusion, respectively. It was found that owing to the packing effect, the porosity and pore size distribution of the pastes were improved; because of the more complete hydration of the superfine slag section, the strength of the mortars increased and had good correlation with the hydration degree of the slag powder calculated.

Keywords: Superfine powder; Packing effect; Dense package; Particle size distribution (PSD); Induced reactivity

1. Introduction

For a long period, the application of granulated blast furnace slag has been confined to the production of slag Portland cement through co-grinding with clinker and gypsum. Because of its less grindability, the surface area of the slag section in commercial cement with surface area of 300 m^2/kg was only 280 m^2/kg [1], and this limited its reactivity. With the development of concrete technology, the concept of superfine powder (defined as powder with particle diameter less than 10 μm) [2] was introduced, and the superfine powder of mineral admixture with a specific surface area of over 500 (usually 800) m^2/kg is now an indispensable part of high-performance concrete (HPC) due to technological and environmental benefits.

The addition of superfine powder, together with superplasticizer, improves the behaviors of concrete considerably. Because of its small size, it functions as filler to improve the pore size distribution and reduce the porosity [3]. Because of its occupation of the space that otherwise would have been occupied by water, more free water is released to upgrade the workability [4,5]. Chemically speaking, smaller particles of slag own greater reactivity to accelerate the pozzolanic effect and the absorption of the abundantly existed calcium hydroxide (25% of the cement hydrates) which is harmful to cement properties.

In this article, the packing effect and pozzolanic effect of superfine slag powder were mathematically analyzed in an effort to evaluate the rudimentary mechanism of the superfine powder quantitatively.

2. Theoretical analysis

2.1. Packing effects

It is well known that porosity is of fundamental importance to many properties of concrete such as strength, permeability, and durability [6,7]. To obtain dense structure in the hardened mortars, the maximization of the dry binder density is a must [8]. Though the calculation of porosity is possible [9], the inconvenience and inaccuracy of the method prohibit its engineering application. Thus, the packing effect is simply elucidated from the standpoint of necessity and possibility.

* Corresponding author. Tel.: +86-10-6277-8206.
E-mail address: niuql00@tsinghua.edu.cu (Q. Niu).

0008-8846/02/$ – see front matter
PII: S0008-8846(01)00730-X

2.1.1. Necessity

The packing density of the commercial cement powder is relatively low because of its narrow particle size distribution (PSD) through closed-circuit grinding process. It could be demonstrated mathematically that cement powder lacks the section of superfine particle compared with the dense packing powder.

2.1.1.1. Size distribution of dense powder and cement powder. The dense package of a powder requires proper PSD described as follows:

$$U_1(D) = 100(D/D_L)^n \quad (1)$$

or

$$U_2(D) = 100\frac{D^n - D_S^n}{D_L^n - D_S^n} \quad (2)$$

Eqs. (1) and (2) are normally called the Andrensen equation [10] and the Dinger–Funk equation [9]. $U(D)$is the weight percent of the dust less in diameter than D, D_L and D_S are the largest and the smallest particle diameter of the powder, n is distribution index.

From their experiments, Andreasen and Andrensen concluded that [10] the packing density of a powder increased with the decrease of the distribution index n, and the greatest packing density occurs when the distribution index n is approaching 1/3, but a much smaller value of n (n<<1/3) is meaningless.

With computer simulation, Dinger and Funk [11] derived a similar conclusion: a powder achieved the greatest packing density when $n = 0.37$.

In fact, when $D = D_S$, $U(D) = 0$ and when $D = D_L$, $U(D) = 100\%$, we know that (Eq. (3)):

$$U(D) = \frac{D^n - D_S^n}{D_L^n - D_S^n} = \frac{(D/D_L)^n - (D_S/D_L)^n}{(D_L/D_L)^n - (D_S/D_L)^n} \quad (3)$$

In other words, Eq. (2) is another edition of Eq. (1) when taking the smallest particle into consideration. They differ only in theoretical sense that the Andrensen equation contains infinitesimal particles that is impossible for actual powder. When D_S is infinitesimal, they are essentially equal. For cement powder with $D_L \approx 100$ μm and $D_S/D_L \approx 0.0001$, the results were similar, e.g, the content of the superfines (<10 μm) from Eqs. (1) and (2) was 46.4% and 43.8%, while that of <20 μm was 58.5% and 56.5%, respectively.

Thus, it could be logically assumed that the greatest packing density existed when the diameter distribution satisfied Eq. (1) and the distribution index n is equal to 1/3.

For the continuous distribution of cement powder, the most frequently used Rosin–Rammler–Bennett (RRSB) equation was given as follows (Eq. (4′)):

$$R(D) = 100\ \exp\left[-\left(\frac{D}{D_e}\right)^n\right] \quad (4)'$$

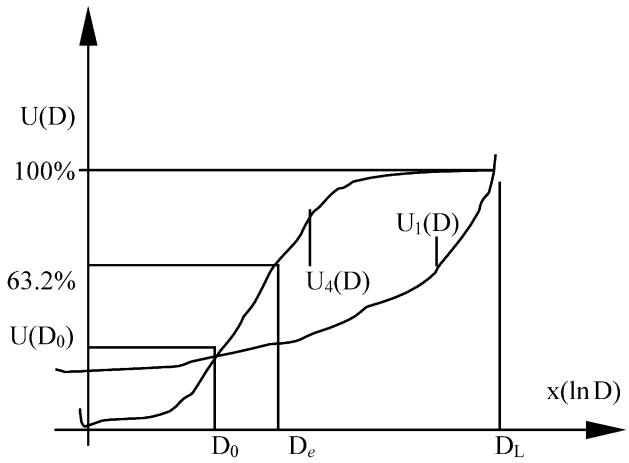

Fig. 1. Schematic comparison of Eq. (4) and Eq. (1).

or

$$U(D) = 100 - R(D) = 100 - 100\ \exp\left[-\left(\frac{D}{D_e}\right)^n\right] \quad (4)$$

In Eq. (4), $R(D)$ is the weight percent of the residue, n is the distribution index and D_e is the characteristic diameter, corresponding to $R(D) = 36.8\%$ or $U(D) = 1 - R(D) = 63.2\%$.

2.1.1.2. Schematic and mathematic comparison. Comparing Eq. (1) with Eq. (4), the actual PSD of cement is quite different from that of the dense packing powder. However, the comparison schematically shown in Fig. 1 indicated that when $D < D_0$, $U_4(D) < U_1(D)$, and when $D > D_0$, $U_4(D) > U_1(D)$.

In Fig. 1, $U_4(D)$ and $U_1(D)$ are the diagrammatic drawing of Eq. (4) (for cement) and Eq. (1) (for dense powder).In logarithmic scale (Eq. (5)),

$$U_1(D) = \exp\left[\ln\left(\frac{D}{D_L}\right)^{\frac{1}{3}}\right] = k_0 e^{\frac{\ln D}{3}} = k_0 e^{\frac{x}{3}},\ k_0 = D_L^{-\frac{1}{3}} \quad (5)$$

This is to say that the content of particles smaller than D_0 in actual powder ($n = 0.85$–1.2) is less than in the dense packing powder. This can be verified mathematically as follows:

Develop Eq. (4) according to the Maclaurin series:

$$\begin{aligned} U_4(D) &= 100\sum_{i=1}^{\infty}\frac{1}{i!}\left(\frac{D}{D_e}\right)^{in} \\ &= 100\left[\left(\frac{D}{D_e}\right)^n - \frac{1}{2!}\left(\frac{D}{D_e}\right)^{2n} + \frac{1}{3!}\left(\frac{D}{D_e}\right)^{3n}\cdots\right] \\ &= 100\left(\frac{D}{D_e}\right)^n\left[1 - \frac{1}{2!}\left(\frac{D}{D_e}\right)^n + \frac{1}{3!}\left(\frac{D}{D_e}\right)^n\cdots\right] \\ &= 100\left(\frac{D}{D_e}\right)^n\alpha \end{aligned}$$

As $0 < \alpha < 1^*$, $U_4(D) < 100(D/D_e)^n$

$$\text{Let } \left(\frac{D}{D_e}\right)^n = \left(\frac{D}{D_L}\right)^{\frac{1}{3}} = \left(\frac{D}{D_e}\right)^{\frac{1}{3}}\left(\frac{D_e}{D_L}\right)^{\frac{1}{3}} = \left(\frac{D}{D_e}\right)^{\frac{1}{3}}\beta$$

$$\text{Then } D = D_e\beta^{\frac{3}{3n-1}} \qquad \beta = \left(\frac{D_e}{D_L}\right)^{\frac{1}{3}} \tag{6}$$

In other words, when $D \le D_e\beta^{(3/(3n-1))}$ (Eq. (7)),

$$U_4(D) < 100\left(\frac{D}{D_e}\right)^n \le U_1(D) = \left(\frac{D}{D_L}\right)^{\frac{1}{3}} \tag{7}$$

For cement powder conforming to RRSB equation (Eq. (4)), when the residue deviation $R(D)$ is taken as 0.0001 or 0.01%,

$$R(D) = 100\ \exp\left[-\left(\frac{D_L}{D_e}\right)^n\right] = 10^{-2}$$

$$\left(\frac{D_L}{D_e}\right)^n = 9.21 \xrightarrow{n=1} \left(\frac{D_e}{D_L}\right)^{\frac{1}{3}} = \beta = 0.477$$

Typically, for cement with $D_e = 30$ μm and $n = 1$, substitute $\beta = 0.477$, $n = 1$ and $D_e = 30$ μm into Eq. (6), we know that

$$D_0 = 9.88\ \mu\text{m} \tag{8}$$

For cement powder with different D_e and different index n, the value of D_0 is different, but there does exist such a threshold diameter below which the percentage of cement powder is less than that of the dense package powder.

* When $D > D_e$, $D/D_e > 1$, $\because\ 0 < U_3(D) = 100(D/D_e)^n\alpha < 100\%$, $\therefore\ 0 < \alpha < 1$.

When $D < D_e$, $D/D_e < 1$, $\because\ 1/i!(D/D_e)^{in} < 1/((i+1)!)(D/D_e)^{(i+1)n}$, $\therefore\ 0 < \alpha < 1$.

From the analysis, we know that the cement powder had high porosity because it lacked fine particles (esp. $\Phi < 10$ μm, as shown in the laser granulometry result of Table 3), therefore, the addition of the superfine powder seems a good answer.

Table 1
The porosity (%) in the Horsfield model

	1st	2nd	3rd	4th	5th	6th
Radius	1	0.414	0.225	0.177	0.116	0^+
Porosity	25.9	20.7	19.0	15.8	14.9	3.9
Number	–	1	2	8	8	∞

All physical and chemical forces such as Van der Waals force, attraction and repulsion forces are neglected.

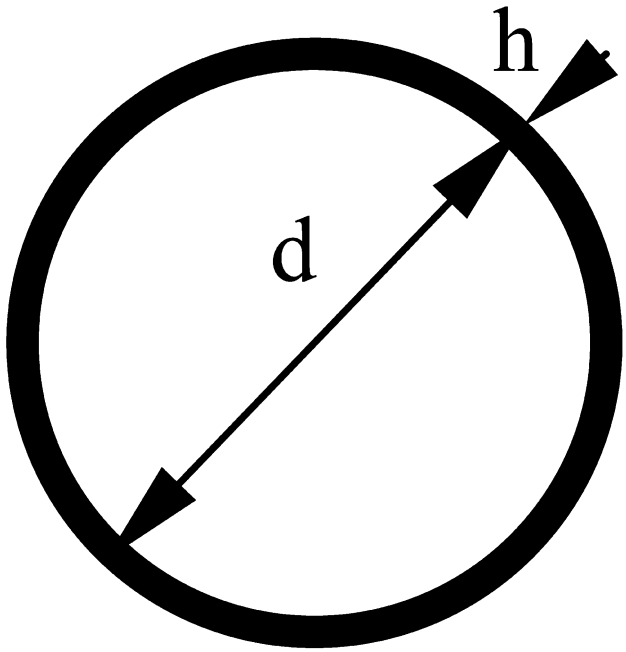

Fig. 2. Hydration model.

2.1.2. Possibility

Let us take a look at the Horsfield model [12]. There existed such assumption that all particles were spherical and those packed at the same time were same-sized. According to the packing sequence, they were named as 1st ball, 2nd ball, and so on. The 1st balls packed according to hexagonal arrangement, leaving a porosity of 25.94%, and the proper-sized 2nd balls joined in the remaining space, . . . The 6th balls were infinitesimal compared with $0.116r$ and were hexagonally packed (porosity is 25.94%), then the final porosity is $0.149 \times 0.259 = 3.9\%$. The result is shown in Table 1.

The model above reveals a fact that with proper diameter distribution, porosity of a powder may be reduced to an ideal level. For powder with mean diameter d_0, the addition of particles less in diameter than $0.414d_0$ and $0.225\ d_0$ may fill into the tetragonal voids and triangular voids existing, and reduce the porosity of the powder.

The superfine powder, with a large amount of this kind of particles, plays a very important role in the reduction of large voids and the decrease of porosity. For cement powder (300 m^2/kg) with a mean diameter of $d_0 = 23.0$ μm, $0.414d_0 = 9.52$ μm, $0.225d_0 = 5.18$ μm. It is known from the measured data (Table 3) that the 500- and 800-m^2/kg slag powders with mean diameters of 9.41 and 5.55 μm were the closest selections and were used in this paper for porosimetry experiment.

2.2. Pozzolanic effect

2.2.1. Mutual enhancement of slag and clinker

Granulated blast furnace slag, as a by-product of iron and steel industry, is formed from cooling of the molten of

Table 2
Composition of clinker and slag

	TiO_2	CaO	SiO_2	Al_2O_3	Fe_2O_3	MgO	C_3S	C_2S	C_3A	C_4AF	SO_3	K[a]	M[b]
Clinker	–	65.58	21.63	5.43	3.34	0.27	57.23	18.84	8.74	10.16	–	–	–
Slag	3.21	33.26	31.47	12.46	2.55	10.99	–	–	–	–	1.37	1.65	1.00

As the basicity $m = 1.0$, the slag is neutral.
[a] $K = (CaO + MgO + Al_2O_3)/(SiO_2 + TiO_2)$.
[b] $M = (CaO + MgO)/(Al_2O_3 + SiO_2)$.

charcoal ash, ironstone impurity and flux such as limestone and dolomite through a water-quenching process. The major chemical compositions are crystallized calcium (magnesium) silicates and calcium (magnesium) aluminum, and the dominating texture is in the glassy phase (>90%). If the molten slag was cooled at a speed slow enough, then mechanically basalt-liked rock will be formed. However, as slag underwent a water-quenching process, 46 kcal/kg (192 kJ/kg) of crystallization heat was preserved, making it a potentially reactive mixture with reactivity lower than the similarly pyroprocessed clinker for its high-SiO_2 and low-CaO content.

Despite all the differences existing between clinker and slag, their major hydration product is C-S-H, though different in Ca/Si ratio (morphology change from fibril to foil is reported in literature as Ca/Si ratio is lower for the product of slag [13]). On the other hand, the Portland cement was alkaline and susceptible to acid erosion. Superfine slag powder could reduce the alkaline and increase the content of C-S-H by absorbing CH in the cement hydrates. The existence of CH accelerated the hydration of slag and the decreased content of $Ca(OH)_2$ enhanced the hydration of C_3S and C_2S, promoting the more rapid and complete hydration of both clinker and slag in cement.

$$2C_3S + 6H \rightarrow C_3S_2H_3 + 3CH$$

$$2C_2S + 4H \rightarrow C_3S_2H_3 + CH$$

$$\text{Slag} + CH \rightarrow C - S - H$$

Table 3
PSD of slag powders with different surface areas

Diameter (μm)	Surface area (m^2/kg) 300	400	500	600	700	800	Dense package
<1	7.13%	9.26%	13.69%	15.59%	18.83%	20.47%	16.7%
<2	11.98%	13.65%	18.36%	26.33%	30.56%	33.21%	21.1%
<3.5	16.57%	18.73%	25.67%	34.44%	39.18%	41.13%	25.4%
<5	20.50%	24.04%	36.46%	41.09%	46.36%	47.8%v	28.6%
<10	30.44%	38.52%	51.52%	56.36%	63.14%	64.12%	36.1%
<20	46.02%	57.08%	70.57%	75.34%	82.50%	82.50%	45.4%
<30	57.74%	67.71%	82.53%	85.75%	91.83%	90.99%	52.0%
<50	74.32%	80.05%	94.53%	95.09%	97.89%	98.18%	57.3%
<80	91.24%	92.81%	99.14%	99.43%	99.71%	99.85%	61.7%
<100	99.6%	99.9%	100%	100%	100%	100%	77.7%
Average	23.1 μm	15.4 μm	9.41 μm	7.68 μm	5.89 μm	5.55 μm	D_L= 213.2 μm

2.2.2. Induced reactivity of slag powder

The concept of "induced reactivity" was introduced to describe the increase of hydration degree with the increase of surface area. From the definition of specific surface area, 1 k of 300 m^2/kg powder owned 300 m^2 of surface area. At a certain hydration depth d_0, the degree of hydration was described as follows:

$$\alpha = 300 d_0 \rho \tag{9}$$

As the surface area was measured with Blaine method, and the method is not suitable for the surface area over 600 m^2/kg, Eq. (9) is not suitable for superfine powder.

The degree of hydration could also be obtained from RRB (Eq. (4)) [14], but for superfine powder, the RRB equation is only a coarse description and the deviation introduced is not negligible. Therefore, the hydration degree of superfine powder should be evaluated in another way.

It is well known that the relationship between the degree of hydration and particle diameter could be expressed as Eq. (10) (see Fig. 2):

$$\alpha = \left[1 - \left(1 - \frac{2h}{d}\right)^3\right] \tag{10}$$

where α is the degree of hydration, h and d are hydration depth and the diameter of the particle.

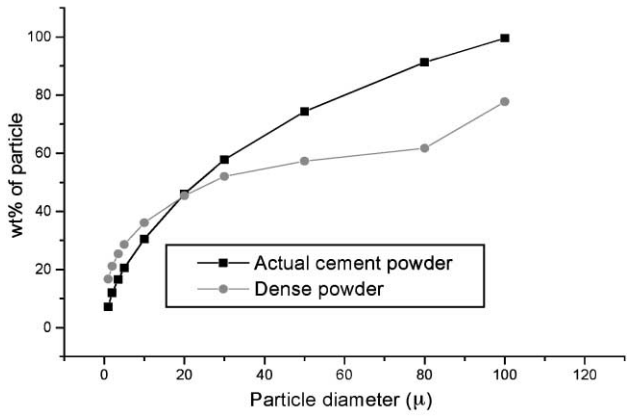

Fig. 3. Comparison of actual cement powder and dense powder.

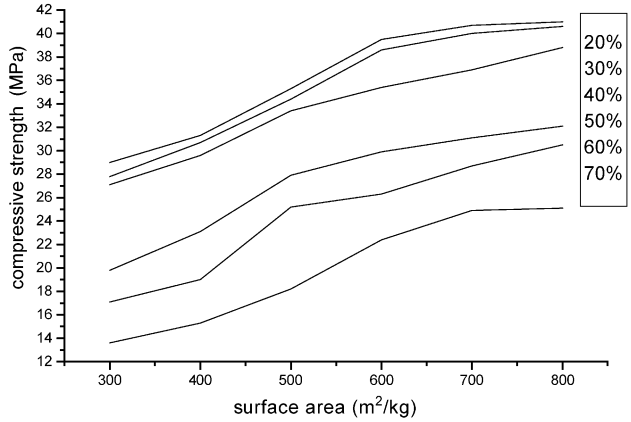

Fig. 4. 3-day compressive strength.

Then, for slag powder, there is the following equation:

$$\alpha = \sum p_i \alpha_i = \sum p_i \left[1 - \left(1 - \frac{2h}{\bar{d}} \right)^3 \right] \quad (11)$$

α_i and P_i are the hydration degree and the weight percentage of the particle between diameter d_i and d_{i+1}, $\bar{d}=(d_i+d_{i+1})/2$, is the average diameter.

As Eq. (11) is a decreasing function, when the hydration depth is constant, the degree of hydration increases with the decrease of average diameter $\bar{d}$. In other words, the finer the powder, the bigger the degree of hydration, and the bigger the induced reactivity.

3. Experiment

3.1. Materials

Rotary kiln clinker and blast furnace slag were used in the experiment. The chemical composition and potential mineral composition of clinker were shown in Table 2. Gypsum with 47% (wt.%) of SO_3 was used as retarder.

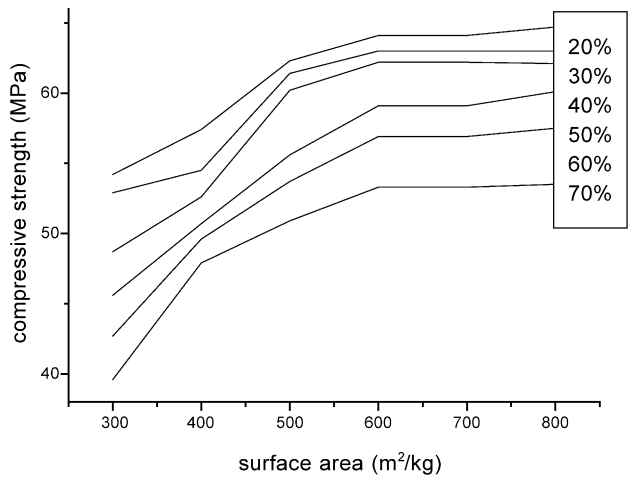

Fig. 5. 28-day compressive strength.

Table 4
The hydration degree α of slag powders

S_b (m²/kg)	300	400	500	600	700	800
α (3 days)	0.127	0.152	0.209	0.249	0.286	0.303
α (28 days)	0.283	0.336	0.46	0.547	0.627	0.66

3.2. Method

Clinker and gypsum were co-ground to produce Portland cement with gypsum content of 3.5% (wt.%). The surface area is 300 m²/kg and the mean diameter is 23.0 μm.

Slag was separately ground to surface area of 300, 400, 500, 600, 700, and 800 m²/kg, then mixed with Portland cement at percentage of 20%, 30%, 40%, 50%, 60%, and 70% as samples, surface area was measured using the Blaine method.

The granulometry of the Portland cement and slag powders was analyzed with a laser granulometer. The W/B ratio and the B/S ratio for the mortars tested for strength were 0.44 and 1:2.5, respectively. Pastes for mercury intrusion was prepared with a W/B ratio of 0.44 and a slag percentage of 40%. The surface area of slag is 500 and 800 m²/kg, with mean diameter of 0.414 and 0.225 time of the cement.

4. Result and discussion

4.1. Particle size distribution, see Table 3

In the last column of Table 3, the PSD of dense package was calculated according to Eq. (1). As shown in Table 3 and the corresponding figure (Fig. 3), the cement powder lacks the particle less in diameter than a threshold D_0 (<20 μm), but the difference in the value of D_0 compared with Eq. (8) shows the considerable difference between theoretic analysis and laser granulometry result.

4.2. Strength

Figs. 4 and 5 show the increase in strength of the mortars as the surface area of the contained slag powder increases.

It is seen from the figures that the compressive strength of cement mortars increases heterogeneously with the increase of the slag surface area. Of the slag powder series,

Table 5
Correlation coefficients (R) between strength and hydration degree at different slag loadings

Dosage	20%	30%	40%	50%	60%	70%
R	0.988	0.993	0.982	0.975	0.957	0.909

the one with surface area of 300 m^2/kg is the least reactive; it functions mainly as diluent in the early stage of hydration. As the slag particle becomes finer, the strength increases at different intervals, the greatest of which appears at 600 m^2/kg for a 3-day compressive strength. For the strength of B, C, and D, the curve concaves, or accelerates at a growing rate before 600 m^2/kg. When the slag percentage is over 50% (E, F, G), the strength of the mortars is relatively low compared with that of B, C, and D because of the lesser content of clinker and the decrease of slag efficiency, since the activating ability of clinker is very important for hydration of slag. However, this trend decreases with the ongoing of hydration. For the 28-day strength, the intervals among different samples with same slag loading diminish to less than 2.1 MPa as the surface area is over 600 m^2/kg.

Table 4 shows the hydration degree of slag powders calculated from the data in Table 3 and Eq. (11) (Hydration depth of slag for 3 and 28 days is 0.05 and 0.25 μm, respectively [15]). It is found that the degree of hydration is closely related to the strength of the mortars. The correlation coefficients of linear regression were shown in Table 5, the decrease in R value at slag dosage of 60% and 70% was partly attributable to the lessening of activating environment for the less content of clinker.

4.3. Porosity

Table 6 shows the porosity of pastes with different slag dosages.

In Table 6, the sample number 5407 is the 7-day paste prepared with cement and 500 m^2/kg slag powder at a percentage of 40%, 5428 is the same sample at the age of 28 days, and so on.

It is seen from the data that, the porosity of the paste number 5407 is 3.0% less than that of the number 3407, the detrimental pores (>100 nm) of pastes 3407 and 5407 account for 22.34% and 13.42% of the total porosity. For the pore over 50 nm, the value is 60.64% to 55.93%, respectively. As the hydration went on and the slag became finer, the porosity of the pastes decreased, e.g., the porosity of paste 8428 is 5.2% less than the paste 5428. In the mean time the pore size distribution is upgraded with the abatement of large pores, which conforms to the analysis in Section 2.1.2.

Table 6
The porosity of pastes (cm^3/g)

Pore size (nm)	#3407	#5407	#5428	#8428
>200	0.0012	0.0015	0	0
100–200	0.0410	0.0229	0	0
50–100	0.0719	0.0774	0.0430	0.0383
20–50	0.0304	0.0313	0.0480	0.0452
5–20	0.0379	0.0418	0.0434	0.0427
<5	0.0054	0.0071	0.006	0.009
Total porosity	0.1876	0.1820	0.1404	0.1331

5. Conclusion

(1) The Horsfield model is a beneficial tool to determine the diameter grade of the superfine powder to optimize the packing effect. The addition of slag powder with surface area of 500 and 800 m^2/kg, and with diameter of 0.414 and 0.225 time of the cement matrix decreases the porosity and improves the pore structure considerably.

(2) With the hydration model and the PSD of the slag powders, the degree of hydration of different powders can be evaluated quantitatively. The calculated results conform perfectly to the strength development of the mortars except when the slag percentage is over 70%.

A.1. About agglomeration

As the particles become smaller, the forces among them increase progressively. As a result, agglomeration appears and the fine particles do not exist as single particle (which is beyond the study of this paper). The agglomeration is especially significant when the diameter of particle is less than 1 μm. For superfine powder however, if used together with a superplasticizer which offsets against flocculation, the result of agglomeration is not taken into consideration in this paper.

A.2. The realization of dense packing of cement powder

The addition of superfine powder according to the Horsfield model does not satisfy the Andrensen equation or the Dinger–Funk equation, therefore, the mixed powder is not the dense packing powder, for the coarse section is more than needed. The widely accepted silica fume is only a second-to-the-best solution, the investigation to realize dense package is expected to minimize the dry porosity.

References

[1] H. Shiyuan, L. Huapu, Green cement and concrete—on the development mode of our national cement and concrete industry, Cement 5th, 1998, pp. 1–5 (in Chinese).
[2] An English–Chinese Dictionary of Science and Technology, Foreign Language Institute, Tsinghua University (Eds). Nation Defense Press, Beijing, 1999.
[3] M. Heikal, H. El-Didamony, M.S. Morsy, Limestone-filled pozzolanic cement, Cem. Concr. Res. 30 (11) (2000) 1827–1834.
[4] M. Nehdi, Why some carbonate filler cause rapid increase of viscosity in dispersed cement-based material, Cem. Concr. Res. 30 (10) (2000) 1663–1669.
[5] A. Kronlöf, Effect of very fine aggregate on concrete strength, material and structure, Cem. Concr. Res. 27 (1) (1994) 15–25.
[6] J. Linhua, G. Yugang, Pore structure and its effect on strength of high-volume fly ash paste, Cem. Concr. Res. 29 (4) (1999) 631–633.
[7] D.P. Bentz, E.J. Garboczi, C.J. Haecker, O.M. Jensen, Effects of cement particle size distribution on performance properties of Portland cement-based material, Cem. Concr. Res. 29 (10) (1999) 1663–1671.
[8] F. Lange, H. Mörtel, V. Ruder, Dense packing of cement pastes and

resulting consequences on mortar properties, Cem. Concr. Res. 27 (10) (1997) 1481–1488.
[9] A.B. Yu, N. Standish, Porosity calculation of multi-component mixture of spherical particles, Powder Technol. 52 (1987) 233–241.
[10] A.M. Andrensen, J. Andrensen, Kolloid Z. 50 (1930) 217.
[11] D.R. Dinger, J.E. Funk, Am. Ceram. Soc. Bull. 68 (8) (1989) 1406.
[12] M.E. Fayed, L. Otten, Handbook of Powder Science and Technology, Chapman & Hall, New York, 1997.
[13] S. Diamond, Hydraulic Cement Pastes: Their Structure and Properties, Cement and Concrete Association, Slough, UK, 1976.
[14] A. Wang, C. Zhang, N. Zhang, The theoretic analysis of the particle size distribution of cement system on the property of cement, Cem. Concr. Res. 29 (11) (1999) 1721–1726.
[15] S. Satowagi, Onishikagero, Hukataniichio, Relationship between slag size and its reactivity, Bull. Cem. Tech. 39 (1985) 49–52 (in Japanese).